Polymer Journal (2019) 51:955–962
https://doi.org/10.1038/s41428-019-0215-2

FOCUS REVIEW

Construction of hydrophilic surfaces with poly(vinyl ether)s and their interfacial properties in water

Yukari Oda[1]

Received: 3 April 2019 / Revised: 8 May 2019 / Accepted: 9 May 2019 / Published online: 10 June 2019

Abstract

We studied the effect of polymer design on the interfacial structure and physical properties of polymer films in water based on a poly(vinyl ether) platform with hydrophilic side-chains to construct bioinert interfaces. Initially, we explored how to prepare hydrophilic surfaces using poly(vinyl ether)s, utilizing the preferential segregation of a rubbery component in a diblock copolymer film with a glassy component, crosslinking a hydrophilic polymer, and designing an interfacial modifier with a special architecture. Characterizing the interfacial structure and physical properties of the obtained polymer films in water revealed that a small difference in the side-chain structure significantly impacts the resultant interfacial properties of the polymers, leading to excellent blood compatibility. Furthermore, we demonstrate that swelling behaviors, which are related to chain dynamics, at the water interface play a key role in determining bioinert properties.

Introduction

Applications of polymeric materials are widely spread in various fields, and the required functionalities are continuously increasing. Particularly in bioapplications, highly functionalized polymers are required, which must meet strict demands and safety standards [1–3]. Such functions, including bioinert properties, are closely related to the structure and dynamics of the polymer chains at the interfaces. Thus, for the development of advanced materials for bioapplications under aqueous conditions, the precise molecular design of polymers is crucial for controlling the interfacial structure in water.

Control of the interfacial structure of polymers has been widely studied thus far. At the surface of a multicomponent polymer film, one component with a lower surface free energy (γ) is segregated to minimize the interfacial free energy with air [4–6]. It is well known that the surface structure of amphiphilic diblock copolymers reorganizes in response to environmental changes [7]. Although γ for polymers is generally considered to be based on the enthalpic factor related to the chemical structure, it also includes an entropic contribution. Thus, it is possible to control the surface structure by entropic-driven surface segregation utilizing the effect of end groups [8, 9] and the unique architectures [10, 11] of polymers. Furthermore, even in a single-component system such as a homopolymer, the interfacial structure can be regulated at the molecular level [12–15]. For instance, for the surface reorganization of poly(methyl methacrylate) (PMMA) in contact with water, the side-chain carbonyl group plays a key role in determining the interfacial structure because it forms hydrogen bonds with water [12, 13]. These findings tell us that precise design considering both enthalpic and entropic contributions to γ should lead to control of the interfacial structure.

For construction of a bioinert interface, a variety of interfacial features should be considered, including surface hydrophilicity [16, 17], hydration states [18–20], and the local dynamics of polymer chains [20–22] at the interfaces. Considering the desired features, we focused on poly(vinyl ether)s with oxyethylene side-chains (POEVEs), especially poly(2-methoxyethyl vinyl ether) (PMOVE) and poly(2-ethoxyethyl vinyl ether) (PEOVE). POEVEs lack a main-chain α-methyl group, increasing their surface hydrophobicity, and a side-chain carbonyl group that forms hydrogen bonds with water at the interface in contrast to poly(meth)acrylates [12–14]. Furthermore, faster chain dynamics can be expected due to the shorter side-chains of PMOVE and PEOVE relative to those of the main-chains of

✉ Yukari Oda
y-oda@cstf.kyushu-u.ac.jp

[1] Department of Applied Chemistry, Kyushu University, 744 Motooka, Nishi-ku, Fukuoka 819-0395, Japan

poly(ethylene oxide) [23]. In spite of such appealing features of POEVEs, preparation of their stable thin films is difficult because they are in a rubbery state at room temperature [24]. Thus, the construction of hydrophilic surfaces with POEVEs is the first objective for our study.

In this work, we examined strategies for the construction of hydrophilic surfaces with well-designed POEVEs and studied the relationship between their interfacial features in water and primary structures to obtain a better understanding of the development of bioinert interfaces. This focus review summarizes our recent results on this work. We start by demonstrating surface segregation of hydrophilic and rubbery POEVEs in a diblock copolymer film. As an alternative method, the preparation of POEVE hydrogel thin films is described. Characterizing the obtained hydrophilic surfaces in water, we discuss some key structural and physical factors for controlling blood compatibility. Finally, we demonstrate the synthesis of an interfacial modifier based on the architectural design of polymers, which can be preferentially segregated at the outermost region in the film due to an entropic contribution, leading to the construction of functional interfaces.

Construction of hydrophilic surfaces based on dynamic-driven segregation: effect of the side-chain structure on blood compatibility

To prepare stable films of rubbery POEVEs, they were connected with glassy poly(cyclohexyl vinyl ether) (PCHVE). Diblock copolymers, poly(CHVE-*b*-MOVE) (CbM) and poly(CHVE-*b*-EOVE) (CbE), were prepared by living cationic polymerization as previously reported in the literature [25, 26]. For comparison, a homopolymer of CHVE (C) was also prepared in the same manner. Figure 1a shows the chemical structures of CbM ($M_n = 62.5$k, $M_w/M_n = 1.06$, $\phi_M = 29\%$), CbE ($M_n = 59.7$k, $M_w/M_n = 1.09$, $\phi_E = 28\%$), and C ($M_n = 43.7$k, $M_w/M_n = 1.05$). M_n and M_w are the number-average and weight-average molecular weights determined by gel permeation chromatography (GPC). ϕ_i is the volume fraction of the i component determined by ^{1}H nuclear magnetic resonance (^{1}H NMR) analysis. Films of CbM, CbE, and C were prepared on silicon substrates by a spin-coating method and then annealed under vacuum at 338 K for 5 h. The film thickness for the polymer films was approximately 60 or 150 nm (only for the platelet adhesion test).

Chemical compositions near the surface in the copolymer films were examined by angular dependent X-ray photoelectron spectroscopy (AD-XPS). The analytical depth of the XPS analysis is given by $3\lambda\sin\theta_e$, where λ and θ_e are the inelastic mean-free path and emission angle of the photoelectrons, respectively. Decreasing θ_e corresponds to a shallower analytical depth. Figure 1b shows the M and E volume fractions (ϕ_M and ϕ_E) for the CbM and CbE films as a function of $\sin\theta_e$. The ϕ_M and ϕ_E values, which were calculated by the integral intensity ratio of the peaks for ether and neutral carbons in the XPS C_{1s} spectra, increased with decreasing $\sin\theta_e$, meaning that the M and E components were enriched at the surface. To evaluate the depth dependence of the volume fraction for M and E in real space, $\phi_i(z)$ was assumed to be expressed by a functional form of a hyperbolic tangent, as shown in equation (1). z refers to the depth.

$$\phi(z) = \phi_\infty + (\phi_s - \phi_\infty) \cdot \left\{1 - \tanh\left(\frac{z - z_i}{d_i/2}\right)\right\}/2 \qquad (1)$$

where ϕ_s, z_i, and d_i are volume fractions at the outermost surface, the thickness of the top layer, and the interfacial width, respectively. Solid and broken curves in panel (b) in Fig. 1 represent the best-fit calculations for the relationship between ϕ_i and $\sin\theta_e$ based on the model depth profiles of $\phi_i(z)$ in close proximity to the surface shown in panel (c) with ϕ_s, z_i, and d_i values of 1.0, 1.1 nm, and 1.1 nm, respectively, for CbM and 1.0, 2.9 nm, and 1.7 nm for CbE. The λ for the C_{1s} photoelectron was estimated to be 3.9 nm [27]. These curves were well superimposed on the experimental data, indicating that M and E were segregated

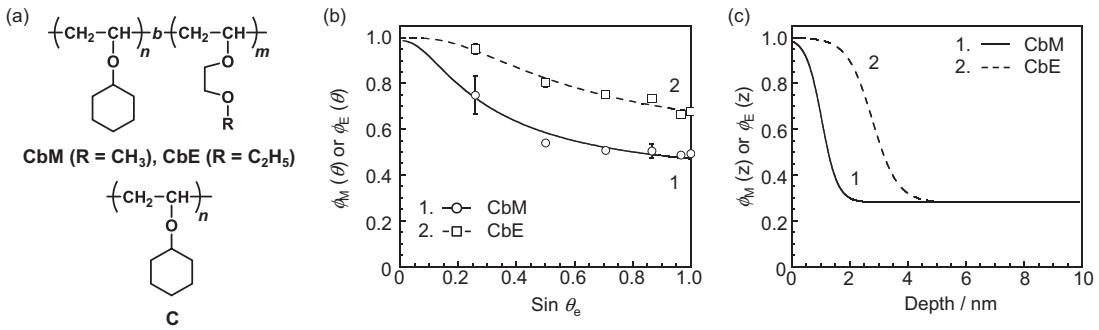

Fig. 1 **a** Chemical structures of CbM (R = CH_3), CbE (R = C_2H_5), and C. **b** Sin θ_e dependence of the volume fractions of M and E for the CbM and CbE films with a thickness of ~60 nm. Open symbols are experimental data, and curves represent the calculated values based on the model composition profiles shown in panel (**c**)

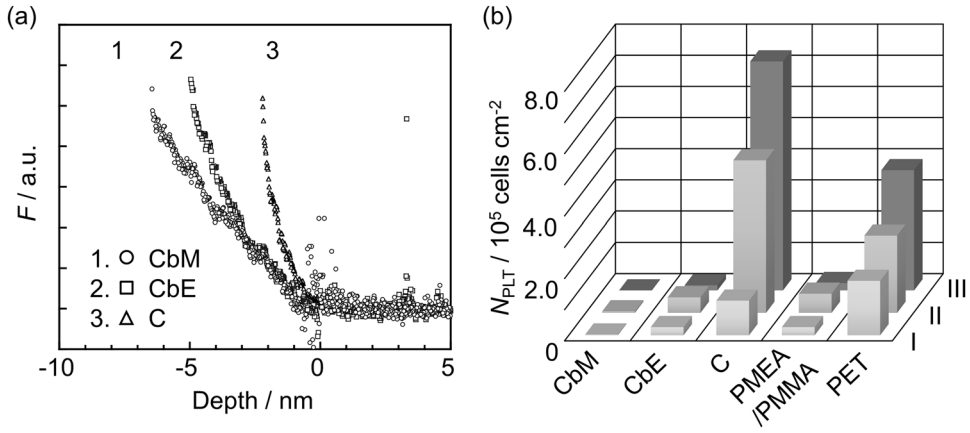

Fig. 2 **a** Force (F) vs. depth curves for the CbM, CbE, and C films measured by AFM with an AC tapping mode in water. **b** The number of platelets adhered (N_{PLT}) and the degree of their activation on CbM, CbE, C, and other reference films. Types I, II, and III refer to the three typical shapes of the adhered platelets: original, partially activated, and strikingly activated, respectively

to cover the outermost surface of the films. The extent of segregation was more striking for CbE than CbM. These results are in good agreement with the relationship among the γ values for each component; γ values for M, E, and C were 30.8, 23.2, and 36.6 mJ m^{-2}, respectively [28]. That is, γ values for rubbery M and E with activated molecular motion decreased due to a larger entropic contribution, and these components in the diblock copolymer films were preferentially segregated in the outermost region, leading to the construction of hydrophilic surfaces [28].

The interfacial features of the obtained hydrophilic surfaces in water were characterized. M and E are water-soluble and insoluble at room temperature, respectively [24]. The aggregation states of the polymer chains at the air and water interfaces were examined using interfacial specific spectroscopy, sum-frequency generation (SFG) vibrational spectroscopy. It was found that the local conformation of the side-chains at the air interface changed when in contact with water for all films, and the manner and extent of the change were dependent on the chemical structures of the side-chains [29]. Such a water-induced conformational change of the chains also resulted in a change in the water structure at the interface. On the diblock copolymers, the water structure became more disordered [29].

The swelling behaviors of the CbM, CbE, and C films near the water interfaces were discussed based on a force-distance measurement using atomic force microscopy (AFM) with an AC tapping mode in water. Panel (a) in Fig. 2 shows the force (F) vs. distance curves obtained for each film in water. F increased with decreasing depth. A depth of zero corresponds to the position where F started to increase. The distance between 0 to the depth where F diverged may correspond to the thickness of the swollen layer at the water interface. In the case of the C film, F acutely increased with decreasing depth, meaning that the interface of C with water was relatively sharp. On the other hand, for diblock copolymers, F gradually increased with decreasing depth, which was more striking for CbM. These results indicated that diblock copolymers formed diffused interfaces and that the thickness of the swollen layer was larger for CbM than CbE. Considering that M is more hydrophilic than E and that both of them were segregated in the outermost region of the films, the results seem to be reasonable.

We then examined the bioinertness of the diblock copolymer films. To evaluate the blood compatibility of the films, a platelet adhesion test was carried out. As negative and positive reference samples, films of poly(2-methoxyethyl acrylate) (PMEA)/PMMA blend [30] and poly(ethylene terephthalate) (PET), respectively, were used. The number of platelets (N_{PLT}) adhered to each sample and their morphologies were examined using scanning electron microscopy. Panel (b) in Fig. 2 shows the N_{PLT} value for each sample, which was classified into three types based on the extent of activation. Types I, II, and III refer to native (round shape), partially activated (showing some pseudopods), and strikingly activated (flat shape with lots of pseudopods), respectively. The N_{PLT} values for CbM and CbE were considerably small and comparable with those for PMEA/PMMA, whereas those for C and PET were quite large. Furthermore, the platelets that adhered to the CbM and CbE films were less activated, whereas those on the C and PET films were highly activated. These results make it clear that the diblock copolymer films significantly suppressed platelet adhesion and activation, which was more obvious for CbM than CbE. Summarizing the findings described above, the interfacial swelling behaviors of polymer chains, inducing faster chain dynamics at the water interface, are significantly related to the achievement of excellent blood compatibility [29].

Control of swelling behaviors by preparation of thin hydrogel films: effect of interfacial physical properties on blood compatibility

Although we succeeded in the construction of excellent bioinert interfaces by designing CbM and utilizing

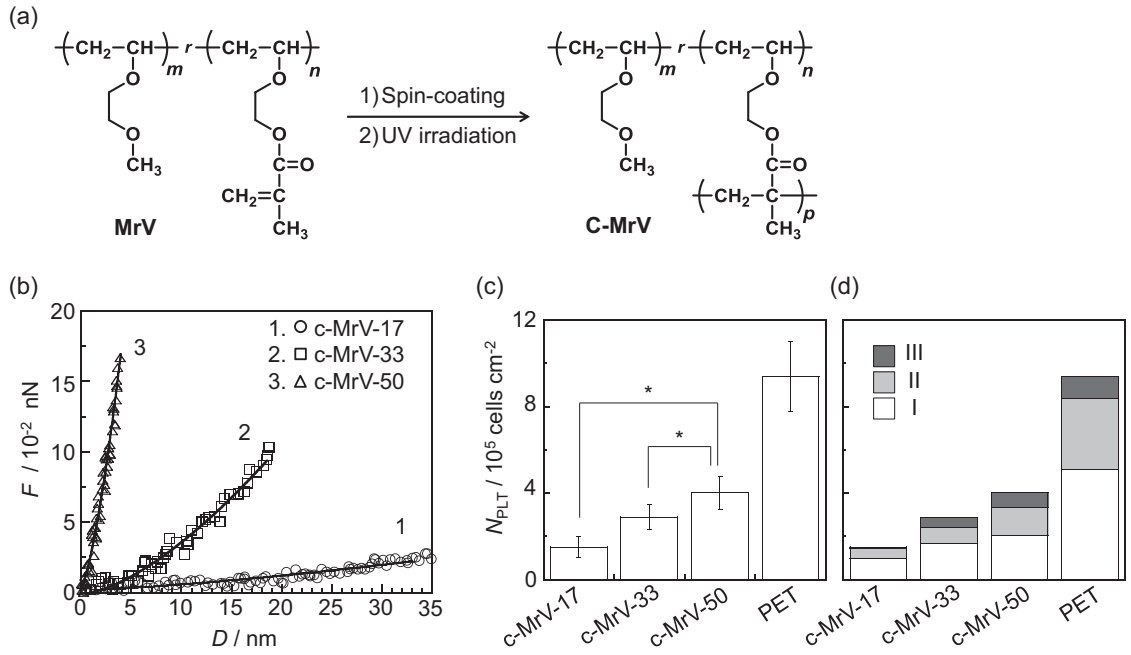

Fig. 3 **a** Chemical structures of MrV and c-MrV. **b** *F* vs. *D* curves for the c-MrV films measured by AFM with a contact mode in water. **c** N_{PLT} values on the c-MrV films and PET film and **d** their classifications based on the extent of activation

segregation behaviors as described above, the outermost region of diblock copolymer thin films can be changed depending on the film thickness [31] and the type of substrate [32]. Therefore, as an alternative way to construct a bioinert PMOVE interface, the preparation of a crosslinked PMOVE film was examined. Its swelling behaviors in water should be dependent on the crosslinking density, so the relationship between the interfacial swelling behaviors and blood compatibility can be further examined without any changes in the side-chain structure of the polymers.

Crosslinked PMOVE films with various crosslinking densities were prepared by living cationic copolymerization of MOVE with 2-(vinyloxy)ethyl methacrylate (VEM) [33–35] by combining subsequent crosslinking reactions. Films of poly(MOVE-*r*-VEM) (MrV) with MOVE:VEM molar ratios of 83:17 (MrV-17), 67:33 (MrV-33), and 50:50 (MrV-50) were prepared on silicon substrates by a spin-coating method. They were irradiated by UV light for the crosslinking reaction at room temperature, soaked in water to remove uncrosslinked chains, and then dried under vacuum at 318 K for 24 h. Figure 3a shows the chemical structures of MrV and crosslinked MrV (c-MrV). Although PMOVE was easily dewetted in the film state and dissolved in water at room temperature, the c-MrV films were stable in air and water. To examine the swelling ratio of the c-MrV films in water, the film thicknesses in air and water were measured by AFM. The original thickness of the films in the dry state was ~185 nm. The swelling ratios of the c-MrV-17, c-MrV-33, and c-MrV-50 films in water were 1.89, 1.44, and 1.27, respectively, at 298 K [36]. Thus, the crosslinking density of c-MrV decreased with the decreasing VEM fraction [36].

The mechanical properties of the c-MrV films near the water interface were examined on the basis of force-distance curve measurements by AFM with a contact mode. Panel (b) in Fig. 3 shows the indentation depth (*D*) dependence of *F* for the films in water acquired using a probe tip with a radius (*r*) of 8 nm. The *D* value is equivalent to the distance from the water interface. *F* increased with increasing *D* for c-MrVs, and the slope of *F* against *D* increased with the increasing VEM fraction. That is, the interface became sharper with the increasing VEM fraction. By applying the Hertz model to the *F*–*D* relationships, the Young's modulus (*E*) was calculated as shown in equation (2) [37–39]:

$$F = \frac{4}{3} \cdot \frac{r^{1/2} \cdot D^{3/2}}{(1-\nu^2)} E \tag{2}$$

where ν is the Poisson's ratio of the film, which is assumed to be 0.5. The solid curves in Fig. 3b represent the best-fit curves. The obtained *E* values were 139 ± 16, 255 ± 15, and 700 ± 37 kPa for c-MrV-17, c-MrV-33, and c-MrV-50, respectively. Thus, with decreasing VEM fraction, *E* decreased, and the swelling ratio increased, as described above.

On the other hand, SFG spectroscopy revealed that the local conformation of the polymer chains for c-MrVs at the water interfaces is almost independent of the VEM fraction.

In addition, the static contact angle against an air bubble in water was ~130° for all c-MrVs. These results indicated that the surface chemistry and aggregation states at the water interface are almost independent of the VEM fraction [36].

To examine the blood compatibility of the c-MrV films, a platelet adhesion test was carried out. Panels (c) and (d) in Fig. 3 show the N_{PLT} values on the c-MrV films and a PET film, as a reference, and their classifications based on the extent of activation. All c-MrV films successfully suppressed platelet adhesion relative to the PET film, and the suppression was clearly dependent on the VEM fraction. The decreasing VEM fraction corresponded well to the increasing swelling ratio as well as decreasing E, resulting in the more significant suppression of the adhesion and activation of platelets. These results revealed that platelet adhesion and activation were more significantly suppressed on the hydrogel films with a more diffused interface [36]. Thus, it can be concluded that the faster chain dynamics at the outermost region of the hydrogel films, which may induce the excluded volume effect, effectively suppress platelet adhesion.

Interfacial modifications based on the segregation of a branched polymer

Finally, we propose a simpler strategy for constructing bioinert surfaces by designing the polymer architecture of poly(vinyl ether)s. A branched polymer can be segregated at the surface in a linear polymer matrix due to the entropic contribution because the chain dimensions are generally smaller for a branched polymer than a linear polymer with similar molecular weights [10]. Thus, by utilizing the surface segregation of the branched polymer, interfacial modifications can be achieved [10, 11, 40].

In this work, as an interfacial modifier to confer bioinert properties, we designed a branched polymer composed of poly[2-(2-ethoxy)ethoxyethyl vinyl ether] (PEOEOVE) graft chains and a PMMA main chain, P(MMA-*g*-EOEOVE), by a combination of living cationic polymerization [26] and atom transfer radical polymerization (ATRP) [41]. Figure 4 shows the synthetic route for P(MMA-*g*-EOEOVE). A PEOEOVE macromonomer containing a terminal methacryloyl group (PEOEOVE-MA) was prepared by typical living cationic polymerization using the 2-(2-ethoxy)ethoxyethyl acetate (EOEOEA)/$Et_{1.5}AlCl_{1.5}$ initiating system in the presence of 1,4-dioxiane in toluene at 223 K [42] and subsequent terminal reaction with 2-hydroxyethyl methacrylate [43]. The terminal reaction qualitatively proceeded and successfully yielded PEOEOVE-MA with a M_n of 3.2k and a M_w/M_n of 1.31. The obtained PEOEOVE-MA and MMA were radically copolymerized by typical conditions for the ATRP of MMA using the ethyl 2-bromoisobutyrate (EtBr*i*Bu)/CuBr initiating/catalyst system in the presence of 4,4′-dinonyl−2,2′-bipyridine in toluene at 363 K [44].

The M_n and M_w/M_n of the obtained P(MMA-*g*-EOEOVE) were 16.8k and 1.66, respectively. The volume fraction of PEOEOVE was determined to be 44% by ^{1}H NMR spectroscopy, meaning that the number of PEOEOVE chains per single P(MMA-*g*-EOEOVE) molecule was calculated to be three [43].

Blend films of P(MMA-*g*-EOEOVE) and PMMA (M_n = 147.5k, M_w/M_n = 1.04) (1/99, 5/95, and 10/90 wt/wt) were prepared on silicon substrates or borosilicate cover glasses by a spin-coating method and were annealed under vacuum

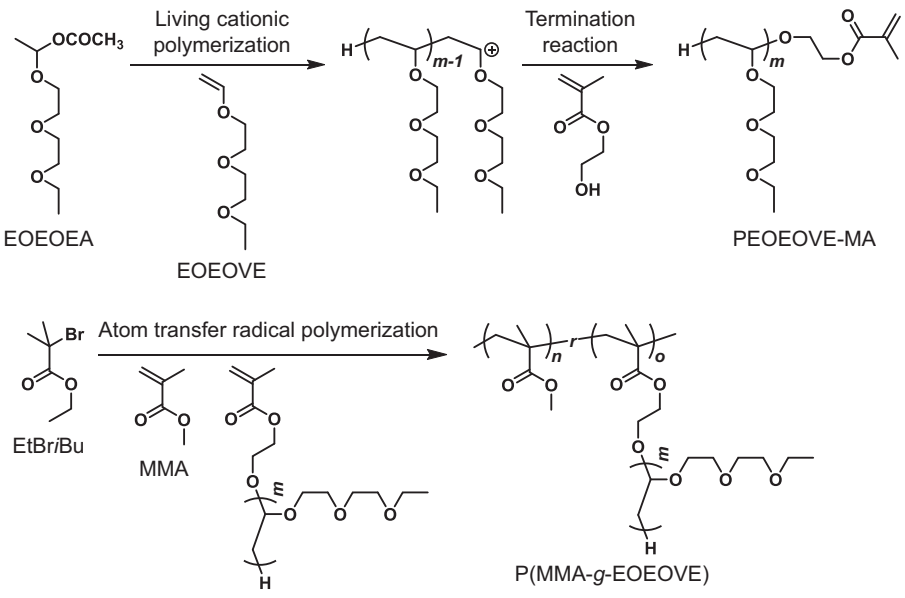

Fig. 4 The synthetic route for P(MMA-*g*-EOEOVE) based on living cationic polymerization in conjunction with atom transfer radical polymerization

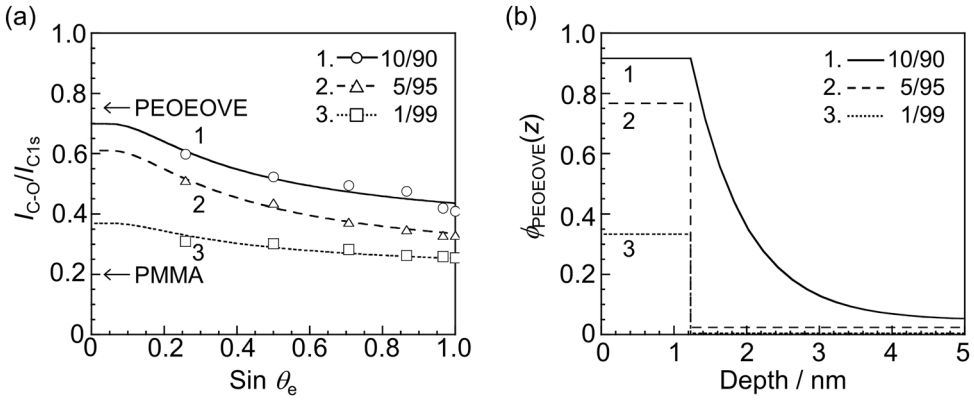

Fig. 5 **a** Sin θ_e dependence of the XPS intensity ratios of the peaks for ether carbon to all carbon (I_{C-O}/I_{C1s}) for the P(MMA-*g*-EOEOVE)/PMMA blend films with a thickness of ~200 nm

at 423 K for 24 h. The thickness of the films was ~200 nm. The root-mean-square roughness of the blend films with the weight ratios of 1/99, 5/95, and 10/90 by AFM was 0.23, 0.23, and 0.28 nm, respectively, indicating that the surfaces of these films were flat and smooth regardless of their blend ratios.

The chemical composition of the blend films near the outermost region was examined by AD-XPS. The λ value for C_{1s} photoelectrons was calculated to be 3.3 nm [27]. The C_{1s} peaks assigned to neutral, ether, and carbonyl carbons were clearly observed at 285.0, 286.5, and 289.0 eV, respectively [43]. Figure 5a shows the sin θ_e dependence of the XPS intensity ratios of the peaks for ether carbon (I_{C-O}) to all carbon (I_{C1s}) for the P(MMA-*g*-EOEOVE)/PMMA blend films. The I_{C-O}/I_{C1s} values increased with an increasing amount of P(MMA-*g*-EOEOVE) and decreasing sin θ_e for all blend films. It can be claimed that P(MMA-*g*-EOEOVE), especially PEOEOVE branches containing more ether carbons than PMMA, was preferentially segregated at the outermost region. Here, the depth dependence of the volume fraction for the PEOEOVE component ($\phi_{PEOEOVE}$) in real space was examined. In the cases of the 1/99 and 5/95 blends, assuming that P(MMA-*g*-EOEOVE) forms a monolayer with PEOEOVE components at the outermost surface, the best-fit curves were superimposed on the experimental data. The curves in panel (a) in Fig. 5 show the best-fit calculations based on the model depth profiles shown in panel (b). Upon increasing the P(MMA-*g*-EOEOVE) content, the surface coverage of PEOEOVE increased without any changes in the thickness of the layer. On the other hand, in the case of the 10/90 blend, another model should be considered to fit the experimental data. It was assumed that once surface coverage with a monolayer of PEOEOVE was almost maximized, the concentration profile beneath the monolayer would follow the mean-field approximation for a miscible polymer blend, that is, exponential decay [27]. Thus, the chemical compositions near the outermost region were dependent on the blend ratio.

As an index for surface modification, the bioinert properties of the blend films were examined by a protein adsorption test. As a model protein, serum albumin was used because it is one of the major components of plasma proteins and is known to attach well on the PMMA surface [45]. The polymer films were immersed into a fluorescein isothiocyanate-labeled bovine serum albumin (FITC-BSA) phosphate-buffer saline (PBS) solution (FITC-BSA: 2 $\mu g \cdot mL^{-1}$) for 1 h at 310 K and then washed with a PBS solution to remove unabsorbed FITC-BSA. The fluorescence intensity from FITC-BSA adsorbed on the films in a PBS solution was monitored by fluorescence microscopy. Figure 6 shows the fluorescent intensity derived from FITC-BSA on the PMMA and P(MMA-*g*-EOEOVE)/PMMA blend films. Although the fluorescence intensity of the 1/99 blend and PMMA films was comparable to each other, that of the 5/95 and 10/90 blend films was lower by ~50–60%. These results indicated that the protein adsorption onto the surfaces was effectively suppressed by mixing 5 or 10 wt% of P(MMA-*g*-EOEOVE) with PMMA. As mentioned above, surface coverage of PEOEOVE was dependent on the blend ratio. Thus, once the surface was effectively covered with hydrophilic PEOEOVE components of P(MMA-*g*-EOEOVE), it exhibited antibiofouling properties due to steric repulsion at the water interface.

Conclusions

In conclusion, we examined the construction of hydrophilic surfaces based on polymer design for bioapplications. Dynamic-driven surface segregation of hydrophilic components in polymer films was demonstrated. Rubbery M and E possess lower γ values due to their activated molecular motion and are preferentially segregated in the outermost region in a diblock copolymer with a glassy C component. Characterizing the outermost region of the obtained polymer films in water, we clearly demonstrated that a small difference in the side-chain structure

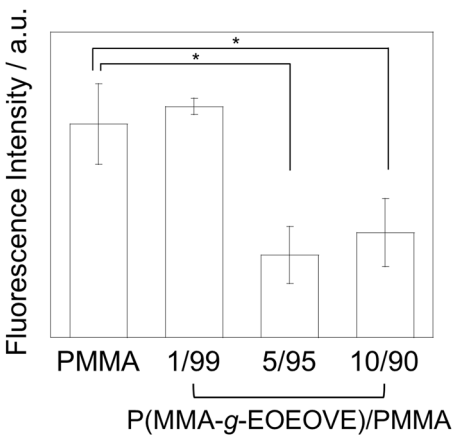

Fig. 6 FITC-BSA adsorption on the PMMA and P(MMA-*g*-EOEOVE)/PMMA blend films. The data represent the mean value ± s.d. $*P < 0.01$ (Student's *t*-test)

significantly impacts the resultant interfacial properties, especially the interfacial swelling behaviors of the polymers, which are closely related to the excellent platelet adhesion behaviors. Furthermore, we proposed a facile method to construct bioinert interfaces by preparing crosslinked PMOVE films. The films were swollen in water, and their interfaces with water became more diffuse with decreasing crosslinking density. The blood compatibility in terms of platelet adhesion on the hydrogel films was better for a more diffuse interface. Finally, a branched polymer containing hydrophilic PEOEOVE was synthesized as an interfacial modifier. The PEOEOVE parts of the branched polymer mixed into PMMA were preferentially segregated in the outermost region of the blend films, leading to an antibiofouling polymer surface. The obtained knowledge presented here will contribute to better polymer design for the development of highly functionalized interfaces.

Acknowledgements The author would like to express sincere gratitude to Prof. Keiji Tanaka, Prof. Hisao Matsuno, and Prof. Daisuke Kawaguchi (Kyushu University) for their continuous encouragement and constructive discussions throughout this work. The author also deeply appreciates great contributions to this work from Dr. Ayanobu Horinouchi, Dr. Cui Zhang, Dr. Shin Sugimoto, Ms. Nozomi Itagaki, and Dr. Hung Kim Nguyen (Kyushu University) and would like to thank Prof. Sadahito Aoshima (Osaka University) and Prof. Shokyoku Kanaoka (The University of Shiga Prefecture) for collaborations. Special thanks to the Asylum Research, Oxford Instruments Company for support. This research was partly supported by JSPS KAKENHI, Grant-in-Aid for Young Scientists (B), Grant Number JP16K17917 and The Mazda Foundation.

Compliance with ethical standards

Conflict of interest The authors declare that they have no conflict of interest.

References

1. Cabral H, Miyata K, Osada K, Kataoka K. Block copolymer micelles in nanomedicine applications. Chem Rev. 2018;118:6844–92.
2. Zhang J, Liu K, Müllen K, Yin M. Self-assemblies of amphiphilic homopolymers: synthesis, morphology studies and biomedical applications. Chem Commun. 2015;51:11541–55.
3. Wei Q, Becherer T, Angioletti-Uberti S, Dzubiella J, Wischke C, Neffe AT, et al. Protein interactions with polymer coatings and biomaterials. Angew Chem Int Ed. 2014;53:8004–31.
4. Hasegawa H, Hashimoto T. Morphology of block polymers near a free surface. Macromolecules. 1985;18:589–90.
5. Russel TP, Coulon G, Deline VR, Miller DC. Characteristics of the surface-induced orientation for symmetric diblock PS/PMMA copolymers. Macromolecules. 1989;22:4600–6.
6. Tanaka K, Takahara A, Kajiyama T. Surface molecular motion in thin films of poly(styrene-block-methyl methacrylate) diblock copolymer. Acta Polym. 1995;46:476–82.
7. Mori H, Hirao A, Nakahama S. Synthesis and surface characterization of hydrophilic-hydrophobic block copolymers containing poly(2,3-dihydroxypropyl methacrylate). Macromolecules. 1994;27:4093–100.
8. Hariharan A, Kumar SK, Russell TP. Reversal of the isotopic effect in the surface behavior of binary polymer blends. J Chem Phys. 1993;98:4163–73.
9. Tanaka K, Takahara A, Kajiyama T. Effect of polydispersity on surface molecular motion of polystyrene films. Macromolecules. 1997;30:6626–32.
10. Yethiraj A. Entropic and enthalpic surface segregation from blends of branched and linear polymers. Phys Rev Lett. 1995;74:2018–21.
11. Walton DG, Soo PP, Mayes AM, Sofia Allgor SJ, Fujii JT, Griffith LG, et al. Creation of stable poly(ethylene oxide) surfaces on poly(methyl methacrylate) using blends of branched and linear polymers. Macromolecules. 1997;30:6947–56.
12. Tateishi Y, Kai N, Noguchi H, Uosaki K, Nagamura T, Tanaka K. Local conformation of poly(methyl methacrylate) at nitrogen and water interfaces. Polym Chem. 2010;1:303–11.
13. Horinouchi A, Atarashi H, Fujii Y, Tanaka K. Dynamics of water-induced surface reorganization in poly(methyl methacrylate) films. Macromolecules. 2012;45:4638–42.
14. Oda Y, Horinouchi A, Kawaguchi D, Matsuno H, Kanaoka S, Aoshima S, et al. Effect of side-chain carbonyl groups on the interface of vinyl polymers with water. Langmuir. 2014;30:1215–19.
15. Dhopatkar N, Anim-Danso E, Peng C, Singla S, Liu X, Joy A, et al. Reorganization of an amphiphilic glassy polymer surface in contact with water probed by contact angle and sum frequency generation spectroscopy. Macromolecules. 2018;51:5114–20.
16. Tamada Y, Ikada Y. Effect of preadsorbed proteins on cell adhesion to polymer surfaces. J Colloid Interface Sci. 1993;155:334–9.
17. Arima Y, Iwata H. Effect of wettability and surface functional groups on protein adsorption and cell adhesion using well-defined mixed self-assembled monolayers. Biomaterials. 2007;28:3047–82.
18. Tanaka M, Motomura T, Kawada M, Anzai T, Kasori Y, Shiroya T, et al. Blood compatible aspects of poly(2-methoxyethylacrylate) (PMEA) relationship between protein adsorption and platelet adhesion on PMEA surface. Biomaterials. 2000;21:1471–81.
19. Hayashi T, Tanaka Y, Koide Y, Tanaka M, Hara M. Mechanism underlying bioinertness of self-assembled monolayers of oligo (ethyleneglycol)-terminated alkanethiols on gold: protein adsorption, platelet adhesion, and surface forces. Phys Chem Chem Phys. 2012;14:10196–206.

20. Seo JH, Kakinoki S, Inoue Y, Nama K, Yamaoka T, Ishihara K, et al. The significance of hydrated surface molecular mobility in the control of the morphology of adhering fibroblasts. Biomaterials. 2013;34:3206–14.
21. Hirata T, Matsuno H, Kawaguchi D, Hirai T, Yamada NL, Tanaka M, et al. Effect of local chain dynamics on a bioinert interface. Langmuir. 2015;31:3661–7.
22. Hirata T, Matsuno H, Kawaguchi D, Inutsuka M, Hirai T, Tanaka M, et al. Dynamics of a bioinert polymer in hydrated states by dielectric relaxation spectroscopy. Phys Chem Chem Phys. 2017; 19:1389–94.
23. Fujii Y, Akabori K, Tanaka K, Nagamura T. Chain conformation effects on molecular motions at the surface of poly(methyl methacrylate) films. Polym J. 2007;39:928–34.
24. Aoshima S, Oda H, Kobayashi E. Synthesis of thermally-induced phase separating polymer with well-defined polymer structure by living cationic polymerization. I. Synthesis of poly(vinyl ether)s with oxyethylene units in the pendant and its phase separation behavior in aqueous solution. J Polym Sci, Part A: Polym Chem. 1992;30:2407–13.
25. Takishita H, Kanazawa A, Kanaoka S, Aoshima S. Design and synthesis of thermo- responsive films with high sensitivity: effects of primary architectures of diblock copolymers and conditions for film formation. Kobunshi Ronbunshu. 2012;69:305–8.
26. Aoshima S, Kanaoka S. A renaissance in living cationic polymerization. Chem Rev. 2009;109:5245–87.
27. Jones RAL, Richards RW. Polymers at surfaces and interfaces. Cambridge: Cambridge University Press; 1999.
28. Zhang C, Oda Y, Kawaguchi D, Kanaoka S, Aoshima S, Tanaka K. Dynamic-driven surface segregation of a hydrophilic component in diblock copolymer films. Chem Lett. 2015;44:166–8.
29. Oda Y, Zhang C, Kawaguchi D, Matsuno H, Kanaoka S, Aoshima S, et al. Design of blood-compatible interfaces with poly(vinyl ether)s. Adv Mater Interfaces. 2016;3:1600034.
30. Hirata T, Matsuno H, Tanaka M, Tanaka K. Surface segregation of poly(2-methoxyethyl acrylate) in a mixture with poly(methyl methacrylate). Phys Chem Chem Phys. 2011;13:4928–34.
31. Knoll A, Horvat A, Lyakhova KS, Krausch G, Sevink GJA, Zvelindovsky AV, et al. Phase behavior in thin films of cylinder-forming block copolymers. Phys Rev Lett. 2002;89:035501.
32. Stoykovich MP, Müller M, Kim SO, Solak HH, Edwards EW, de Pablo JJ, et al. Directed assembly of block copolymer blends into nonregular device-oriented structures. Science. 2005;308:1442–6.
33. Aoshima S, Hasegawa O, Higashimura T. Living cationic polymerization of vinyl ethers with a functional group. 2. Polymerization of vinyl ethers with an unsaturated ester pendant. Polym Bull. 1985;13:229–35.
34. Sugihara S, Ohashi M, Ikeda I. Synthesis of fine hydrogel microspheres and capsules from thermoresponsive coacervate. Macromolecules. 2007;40:3394–401.
35. Sakaguchi T, Ohashi M, Shimada K, Hashimoto T. Synthesis and gas permeability of membranes of poly(vinyl ether)s bearing oxyethylene segments. Polym (Guildf). 2012;53:1659–64.
36. Itagaki N, Oda Y, Hirata T, Nguyen HK, Kawaguchi D, Matsuno H, et al. Surface characterization and platelet adhesion on thin hydrogel films of poly(vinyl ether). Langmuir. 2017;33: 14332–39.
37. Sneddon IN. The relation between load and penetration in the axisymmetric boussinesq problem for a punch of arbitrary profile. Int J Eng Sci. 1965;3:47–57.
38. Johnson KL, Greenwood JA. An adhesion map for the contact of elastic spheres. J Colloid Interface Sci. 1997;192:326–33.
39. Nakajima K, Ito M, Wang D, Liu H, Nguyen HK, Liang X, et al. Nano-palpation AFM and its quantitative mechanical property mapping. Microscopy. 2014;63:193–208.
40. Atarashi H, Ariura F, Akabori K, Tanaka A, Ozawa M, Tanaka K, et al. Interfacial segregation of hyper-branched polystyrene in mixtures of linear component. Trans Mater Res Soc Jpn. 2007;32: 231–4.
41. Matyjaszewski K, Tsarevsky NV. Macromolecular engineering by atom transfer radical polymerization. J Am Chem Soc. 2014;136: 6513–33.
42. Aoshima S, Sugihara S. Syntheses of stimuli-responsive block copolymers of vinyl ethers with side oxyethylene groups by living cationic polymerization and their thermosensitive physical gelation. J Polym Sci Part A: Polym Chem. 2000;38:3962–5.
43. Sugimoto S, Oda Y, Hirata T, Matsuyama R, Matsuno H, Tanaka K. Surface segregation of a branched polymer with hydrophilic poly[2-(2-ethoxy)ethoxyethyl vinyl ether] side chains. Polym Chem. 2017;8:505–10.
44. Grimaud T, Matyjaszewski K. Controlled/"living" radical polymerization of methyl methacrylate by atom transfer radical polymerization. Macromolecules. 1997;30:2216–8.
45. Hasegawa M, Kitano H. Adsorption kinetics of proteins onto polymer surfaces as studied by the multiple internal reflection fluorescence method. Langmuir. 1992;8:1582–6.

Yukari Oda received her BS (2006), MS (2008), and PhD (2011) degrees from Osaka University under the supervision of Professor Sadahito Aoshima. In 2010–2011, she has also been to University of Michigan as a Visiting Scholar to work with Professor Kenichi Kuroda for eight months. From 2011 to 2013, she worked as a Specially Appointed Researcher with Professor Aoshima at Osaka University. In April 2013, she moved to Department of Applied Chemistry, Kyushu University as a Research Assistant Professor to work with Professor Keiji Tanaka and was promoted to an Assistant Professor in September 2016. She received Award for Encouragements of Research in Polymer Science from The Society of Polymer Science, Japan in 2018. Her current research interests include construction of functional polymer interfaces and structural analysis of polymer interfaces.